J Stat Phys (2008) 130: 1047–1062
DOI 10.1007/s10955-007-9475-x

From Symmetry Breaking to Poisson Point Process in 2D Voronoi Tessellations: the Generic Nature of Hexagons

Valerio Lucarini

Received: 7 August 2007 / Accepted: 13 December 2007 / Published online: 3 January 2008

Abstract We bridge the properties of the regular triangular, square, and hexagonal honeycomb Voronoi tessellations of the plane to the Poisson-Voronoi case, thus analyzing in a common framework symmetry breaking processes and the approach to uniform random distributions of tessellation-generating points. We resort to ensemble simulations of tessellations generated by points whose regular positions are perturbed through a Gaussian noise, whose variance is given by the parameter α^2 times the square of the inverse of the average density of points. We analyze the number of sides, the area, and the perimeter of the Voronoi cells. For all values $\alpha > 0$, hexagons constitute the most common class of cells, and 2-parameter gamma distributions provide an efficient description of the statistical properties of the analyzed geometrical characteristics. The introduction of noise destroys the triangular and square tessellations, which are structurally unstable, as their topological properties are discontinuous in $\alpha = 0$. On the contrary, the honeycomb hexagonal tessellation is topologically stable and, experimentally, all Voronoi cells are hexagonal for small but finite noise with $\alpha < 0.12$. For all tessellations and for small values of α, we observe a linear dependence on α of the ensemble mean of the standard deviation of the area and perimeter of the cells. Already for a moderate amount of Gaussian noise ($\alpha > 0.5$), memory of the specific initial unperturbed state is lost, because the statistical properties of the three perturbed regular tessellations are indistinguishable. When $\alpha > 2$, results converge to those of Poisson-Voronoi tessellations. The geometrical properties of n-sided cells change with α until the Poisson-Voronoi limit is reached for $\alpha > 2$; in this limit the Desch law for perimeters is shown to be not valid and a square root dependence on n is established. This law allows for an easy link to the Lewis law for areas and agrees with exact asymptotic results. Finally, for $\alpha > 1$, the ensemble mean of the cells area and perimeter restricted to the hexagonal cells agree remarkably well with the full ensemble mean; this reinforces the idea that hexagons, beyond their ubiquitous numerical prominence, can be interpreted as *typical* polygons in 2D Voronoi tessellations.

V. Lucarini (✉)
ADGB—Department of Physics, University of Bologna, Viale Berti Pichat 6/2, 40127 Bologna, Italy
e-mail: lucarini@adgb.df.unibo.it

V. Lucarini
CINFAI, Via Viviano Venanzi 15, 62032 Camerino, Italy

Keywords Voronoi tessellation · Topological stability · Random geometry · Symmetry breaking · Poisson point process · Desch law · Lewis law · Gaussian noise

1 Introduction

Given a set X of discrete points in the Euclidean plane, for almost any point a in the plane there is one specific point $x_i \in X$ which is closest to a. The set of all points of the plane which are closer to a given point $x_i \in X$ than to any other point $x_j \neq x_i, x_j \in X$, is the interior of a convex polygon usually called the Voronoi cell for x_i. The set of the polygons Π_i, each corresponding to (and containing) one point $x_i \in X$, is the Voronoi tessellation corresponding to X, and provides a partitioning of the plane [35, 36]. As well known, the Delaunay triangulation gives the dual graph of the Voronoi tessellation [10]. Voronoi tessellation can be defined for general N-dimensional Euclidean spaces, and extensions to the case of non-Euclidean spaces have also been provided [27].

Since the Voronoi tessellation creates a one-to-one optimal—in the sense of shortest distance—correspondence between a point and a polytope, 2D and 3D Voronoi tessellations have long been considered for applications in several research areas, such as telecommunications [30], biology [15], astronomy [22], forestry [4] atomic physics [17], metallurgy [38], polymer science [12], materials science [6]. In solid-state physics, the Voronoi cells of the single component of a crystal are known as Wigner-Seitz cells [1, 5]. In a geophysical context, Voronoi tessellations have been widely used to analyze spatially distributed observational or model output data [34]. In particular, they are a formidable tool for performing arbitrary space integration of sparse data, without adopting the typical procedure of adding spurious information, as in the case of linear or splines interpolations [25]. Actually, it was this context that Thiessen and Alter, with the purpose of computing river basins water balance from irregular and sparse rain observations, discovered independently for the 2D case the tessellation introduced by Voronoi just few years earlier [33]. Moreover, a connection has been recently established between the Rayleigh-Bènard convective cells and Voronoi cells, with the hot spots (locations featuring the strongest upward motion of hot fluid) of the former basically coinciding with the points *generating* the Voronoi cells, and the locations of downward motion of cooled fluid coinciding with the sides of the Voronoi cells [28].

The quest for achieving low computational cost for actually evaluating the Voronoi tessellation of a given discrete set of points X is ongoing and involves an extensive research performed within various scientific communities [3, 7, 18, 31, 37]. The theoretical investigation of the statistical properties of general N-dimensional Voronoi tessellations has proved to be a rather hard task, so that direct numerical simulation is the most extensively adopted investigative approach. For a review of the theory and applications of Voronoi tessellations, see [2, 27].

A great deal of theoretical and computational work has focused on the more specific and tractable problem of studying the statistical properties of Poisson-Voronoi tessellations. These are Voronoi tessellations obtained starting from a random set of points X generated as output of a homogeneous Poisson point process. This problem has a great relevance at practical level because it corresponds, *e.g.*, to studying crystal aggregates with random nucleation sites and uniform growth rates. Exact results concerning the mean statistical properties of the interface area, inner area, number of vertices, etc. of the Voronoi cells have been obtained for general Euclidean spaces [8, 9, 13, 14, 26]. Recently, some important results have been obtained for the 2D case [20]. The results of direct numerical investigations have been found in agreement with the theoretical findings, and, moreover, have shown that both 2-parameter [23] and 3-parameter [21] gamma distributions fit up to a high degree of accuracy

the empirical pdfs of the number of vertices, of the perimeter and of the area of the cells. Very extensive and more recent calculations have basically confirmed these results [32]. In spite of several attempts, the *ab-initio* derivation of the pdfs of the geometrical properties of Poisson-Voronoi tessellations has not been yet obtained, except in asymptotic regimes [19]. Nevertheless, it is interesting, and somewhat confusing, to note that the asymptotic results regarding the statistics of the number of sides of the cells are not compatible with the gamma distribution family.

In recent years, various studies have focused on the geometrical properties of Voronoi tessellations resulting from non strictly Poissonian random processes. In particular, given the obvious relevance in terms of applications, such as for packaging problems, a great deal of attention has been directed towards tessellations resulting from points which are randomly distributed in the space and are subjected to a minimal point-to-point distance δ—a sort of hard-core nuclei hypothesis [29, 39]. Whereas the $\delta = 0$ case corresponds to the Poisson-Voronoi situation, it is observed that by increasing δ the *degree of randomness* of the tessellation is decreased—the pdfs of the statistical properties of the geometrical characteristics become more and more peaked—until for a certain critical δ-value a regular tessellation, which in the 2D case is the hexagonal honeycomb one, is obtained. In any case, it is found that the gamma distributions provide excellent fits for a very large range of values of δ [39].

In this paper we want to explore a somewhat different problem of parametric dependence of the Voronoi tessellation statistics. We start from three regular polygonal tessellations of the plane, the honeycomb hexagonal, the square, and triangular tessellations. They are obtained by setting the points x_i as vertices of regular triangles, squares, and hexagons, respectively. Using an ensemble-based approach, we study the break-up of the symmetry of the three systems and quantitatively evaluate how the statistical properties of the geometrical characteristics of the resulting 2D Voronoi cells change when we perturb with a spatially homogeneous Gaussian noise of increasing intensity the positions of the points x_i. Our paper is organized as follows. In Sect. 2 we describe the methodology of work and the set of numerical experiments performed. In Sect. 3 we show our results. In Sect. 4 we present our conclusions and perspectives for future work.

2 Data and Methods

2.1 Scaling Properties of Voronoi Tessellations

Let's first consider a homogeneous Poisson point process Ψ generating as output a random set of points X in the Euclidean plane such that the expectation value for the number of points x_i belonging, without loss of generality, to a square region Γ is $\rho_0|\Gamma| = \rho_0 R^2$, where ρ_0 is the intensity of the process, $|\Gamma|$ is the measure of Γ and R is the side of the square. The fluctuations are of the order of $\sqrt{\rho_0|\Gamma|} = \sqrt{\rho_0}R$. If $\rho_0|\Gamma| \gg 1$, we are in the thermodynamic limit and the number of Voronoi cells inside Γ is $N_V \approx \rho_0|\Gamma|$, so that boundary effects are negligible. The point density ρ_0 can thus be scaled to unity, or, alternatively, the domain can be scaled to the square $\Gamma_1 = [0, 1] \times [0, 1]$. We will stick to the second perspective. Theoretical results suggest that the ensemble mean—where the statistics is computed over all realizations of the random process—of the number of sides of the Voronoi cells inside Γ is $\langle \mu(n)|_{PV} \rangle = 6$ (PV indicates Poisson-Voronoi), which agrees with the general Euler's theorem on planar graphs with trivalent vertices. Moreover, the ensemble mean of the area of the Voronoi cell is $\langle \mu(A)|_{PV} \rangle = 1/\rho_0$, and the ensemble mean of the perimeter of a

Voronoi cell is $\langle \mu(P)|_{PV} \rangle = 4/\sqrt{\rho_0}$. Therefore, the ensemble mean statistical properties of the Poisson-Voronoi tessellation are intensive, as they depend on the intensive parameter ρ_0. For clarity's sake, we specify that the expression $\mu(Y)$ ($\sigma(Y)$) refers to the mean value (standard deviation) of the variable Y over the ρ_0 cells for the single realization of the random process. The expression $\langle E \rangle$ ($\delta[E]$), instead, indicates the ensemble mean (standard deviation) of the random variable E.

We then consider a random point process Φ generating a spatially periodic distribution of points x_i in the plane, where the discrete translational symmetry is generated by the lattice vectors $\vec{v}_1$ and $\vec{v}_2$. If $R \gg |\vec{v}_1|, |\vec{v}_2|$, the expectation value of the number of x_i's belonging to a square region Γ, independently of its position in the plane, can also be expressed as $\rho_0|\Gamma| = \rho_0 R^2$, where ρ_0 is the coarse-grained intensity of the process. Also in this case, we can assume the thermodynamic approximation and rescale our domain to the square $\Gamma_1 = [0, 1] \times [0, 1]$, with $1 \gg |\vec{v}_1|, |\vec{v}_2|$ and $\rho_0 \gg 1$. Using scaling arguments, one obtains that for these processes, $\langle \mu(A) \rangle, \langle \sigma(A) \rangle \propto 1/\rho_0$ and $\langle \mu(P) \rangle, \langle \sigma(P) \rangle \propto 1/\sqrt{\rho_0}$, where the proportionality constants depend on the specific process considered. Therefore, by multiplying the ensemble mean estimators of the mean and standard deviation of the area (perimeter) of the Voronoi cells times ρ_0 ($\sqrt{\rho_0}$), we obtain universal functions.

2.2 Simulations

As a starting point, we consider the three regular tessellations of the plane. These are special cases of the above-mentioned Φ random periodic point processes where the distribution of points is given by a collection of Dirac's delta's, each centered in a point x_i belonging to a regular grid.

If we consider a regular square grid of points x_i with sides $l = |\vec{v}_1| = |\vec{v}_2|, \vec{v}_1 \perp \vec{v}_2$, the Voronoi cell Π_i corresponding to x_i is given by the square centered in x_i with the same side length and orientation as the x_i grid, so that the grid of the vertices y_i of the tessellation is translated with respect to the x_i grid by $l/2$ in both orthogonal directions (the verse is not relevant). Therefore, the vertices of the Voronoi tessellation resulting from the points y_i are nothing but the initial points x_i. If $l = l_S = 1/\sqrt{\rho_0} = |\vec{v}_1| = |\vec{v}_2|$, we will have ρ_0 points—and ρ_0 corresponding square Voronoi cells—in $\Gamma_1 = [0, 1] \times [0, 1]$. Similarly, a regular hexagonal honeycomb tessellation featuring ρ_0 points and ρ_0 corresponding regular Voronoi cells in $\Gamma_1 = [0, 1] \times [0, 1]$ is obtained by using a grid of points x_i set as regular triangles with sides $l_T = \sqrt{2/(\sqrt{3}\rho_0)} = |\vec{v}_1| = |\vec{v}_2|$, where the angle between $\vec{v}_1$ and $\vec{v}_2$ is 60°. Finally, the regular triangular tessellation featuring a density ρ_0 of Voronoi cells derives from a regular grid of points x_i set as hexagons with sides $l_H = \sqrt{4/(3\sqrt{3}\rho_0)} = |\vec{v}_1|/\sqrt{3} = |\vec{v}_2|/\sqrt{3}$, again with an angle of 60° between the $\vec{v}_1$ and $\vec{v}_2$. Therefore, the regular hexagonal and the regular triangular tessellation are conjugate via Voronoi tessellation.

For all regular grids, we introduce a symmetry-breaking 2D-homogeneous ε-Gaussian noise, which randomizes the position of the points x_i about their deterministic positions with a spatial variance $|\varepsilon^2|$. We define $|\varepsilon^2| = \alpha^2 l_S^2 = \alpha^2/\rho_0$, thus expressing the mean squared displacement as a fraction α^2 of the inverse of the density of points, which is the natural squared length scale. In all cases, when ensembles are considered, the probability distribution of the points x_i is still periodic.

By definition, if $\alpha = 0$ we are in the deterministic case. We study how the statistical properties of n, P, and A of the Voronoi cells change with α, covering the whole range going from the symmetry breaking, occurring when α becomes positive, up to the progressively more and more uniform distribution of x_i, obtained when α is large with respect to 1, so

that the distributions of nearby points x_i overlap more and more significantly. We then perform our statistical analyses by considering $M = 1000$ members of the ensemble of Voronoi tessellations generated for each value of α ranging from 0 to 5 with step 0.01. The actual simulations are performed by using, within a customized routine, the MATLAB7.0® function voronoin.m, which implements the algorithm introduced by Barber et al. [3], to a set of points x_i having density $\rho_0 = 10000$. Tessellation has been performed starting from points x_i belonging to the square $[-0.2, 1.2] \times [-0.2, 1.2] \supset \Gamma_1 = [0, 1] \times [0, 1]$, but only the cells belonging to Γ_1 have been considered for evaluating the statistical properties, in order to limit density depletion in the case of large values of α due to one-step Brownian diffusion of the points nearby the boundaries.

The distributions of n, P, and A are then fitted using a 2-parameter gamma distribution with the MATLAB7.0® function gammafit.m, which implements a maximum likelihood method.

3 Results

We expect that the exploration of the parametric range from $\alpha = 0$ to $\alpha = 5$ should allow us to join on the two extreme situations of perfectly deterministic, regular tessellation, to the tessellation resulting from a set of points X generated with a Poisson point process.

In the deterministic $\alpha = 0$ case, it is easy to deduce the properties of the Voronoi cells from basic Euclidean geometry. In all three cases, our construction implies $\rho_0 \mu(A)|_{\alpha=0} = 1$. For square tessellation, we have $\mu(n)|_{\alpha=0} = 4$, $\sqrt{\rho_0}\mu(P)|_{\alpha=0} = 4$, where the α-dependence of the statistical properties is indicated. For honeycomb tessellation, we have $\mu(n)|_{\alpha=0} = 6$ and $\sqrt{\rho_0}\mu(P)|_{\alpha=0} = \sqrt{24/\sqrt{3}}$, whereas, for triangular tessellation, we have $\mu(n)|_{\alpha=0} = 3$ and $\sqrt{\rho_0}\mu(P)|_{\alpha=0} = \sqrt{36/\sqrt{3}}$. In all three cases, given the regular pattern in space, all cells are alike, and given the deterministic nature of the tessellation, there are no fluctuations within the ensemble.

3.1 Number of Sides of the Cells

In the case of the regular square tessellation, the introduction of a minimal amount of symmetry-breaking noise induces a transition in the statistics of $\mu(n)|_\alpha$ and $\sigma(n)|_\alpha$, since $\langle \mu(n)|_\alpha \rangle$ and $\langle \sigma(n)|_\alpha \rangle$ are discontinuous in $\alpha = 0$. In Figs. 1a–1b we plot the functions $\langle \mu(n)|_\alpha \rangle$ and $\langle \sigma(n)|_\alpha \rangle$; the half-width of the error bars are twice the corresponding values of $\delta[\mu(n)|_\alpha]$ and $\delta[\sigma(n)|_\alpha]$, whereas the Poisson-Voronoi values are indicated for reference. We have that $\langle \mu(n)|_{\alpha=0} \rangle = 4 \neq 6 = \langle \mu(n)|_{\alpha=0^+} \rangle$, where with $\alpha = 0^+$ we indicate the right limit to 0 with respect to the parameter α, obtained numerically by considering very small positive values of the parameter α. The regular square tessellation results to be structurally unstable, as the introduction of noise breaks the special quadrivalent nature of the vertices of the Voronoi cells and drives the system to the generic behavior described by Euler's theorem. Moreover, $\langle \sigma(n)|_{\alpha=0} \rangle = 0 \neq 0.93 \approx \langle \sigma(n)|_{\alpha=0^+} \rangle$, which shows that the width of the distribution of the number of sides is finite also for infinitesimal noise. The ensemble fluctuations $\delta[\mu(n)|_\alpha]$ and $\delta[\sigma(n)|_\alpha]$ are discontinuous functions in $\alpha = 0$, since they reach a finite positive value as soon as the noise is switched on. Considering larger values of α, we have that $\langle \sigma(n)|_\alpha \rangle$ is numerically almost constant (within few percents) up to $\alpha \approx 0.35$, where its value begins to quickly increase before reaching the asymptotic value $\langle \sigma(n)|_\alpha \rangle \approx 1.33$ for $\alpha > 2$, which essentially coincides with what obtained in the Poisson-Voronoi case. The

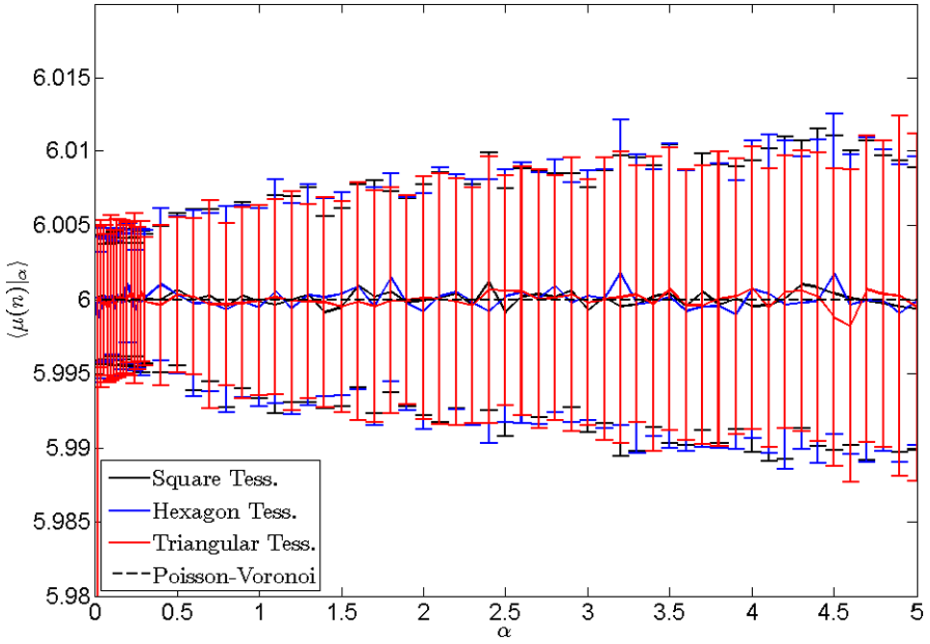

(a)

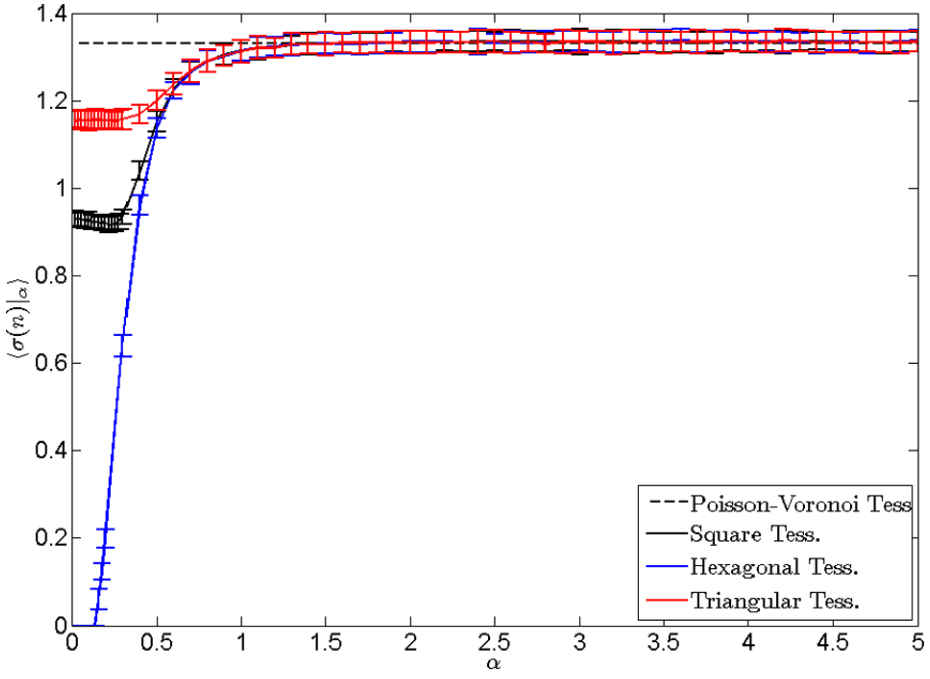

(b)

Fig. 1 (Color online) Ensemble mean of the mean: (**a**) and of the standard deviation; (**b**) of the number of sides (n) of the Voronoi cells. Note that in (**a**) the number of sides of all cells is 4 (3) out of scale—for $\alpha = 0$ in the case of regular square (triangular) tessellation. Half-width of the error bars is twice the standard deviation computer over the ensemble. Poisson-Voronoi limit is indicated

function $\langle \mu(n)|_\alpha \rangle$ is, in agreement with Euler's law, constant within few permils around the value of 6 for all $\alpha > 0$, so that the mean topological charge is zero. These results suggest that, topologically speaking, the *route to randomness* from the square regular tessellation to the Poisson-Voronoi case goes through a finite range $0 < \alpha < 0.35$, where the statistical properties of the topology of the cells are rather stable. Moreover, in this range, hexagons dominate and their fraction is almost constant (within few percents), whereas for larger values of α, the fraction of hexagon declines but is still dominant (not shown).

Similarly, the triangular tessellation results to be unstable: we have that $\langle \mu(n)|_{\alpha=0} \rangle = 3 \neq 6 = \langle \mu(n)|_{\alpha=0^+} \rangle$ and $\langle \sigma(n)|_{\alpha=0} \rangle = 0 \neq 1.17 \approx \langle \sigma(n)|_{\alpha=0^+} \rangle$, and again the ensemble fluctuations $\delta[\mu(n)|_\alpha]$ and $\delta[\sigma(n)|_\alpha]$ are discontinuous functions in $\alpha = 0$. As expected, for all values $\alpha > 0$, $\langle \mu(n)|_\alpha \rangle = 6$, with hexagons being the dominant class of polygons. The introduction of an infinitesimal noise destroys the peculiar hexagonal nature of the vertices of the Voronoi cells and makes the system obey the Euler's theorem. Also in this case, we find a finite range $0 < \alpha < 0.45$—slightly wider than for the square tessellation—such that $\langle \sigma(n)|_\alpha \rangle$ and the fraction of hexagons, are numerically almost constant. This property seems to define robustly a topologically quasi-stable weakly perturbed state.

When considering the regular hexagonal honeycomb tessellation, the impact of introducing noise in the position of the points x_i is quite different from what previously observed. Results are also shown in Figs. 1a–1b. The first feature is that an infinitesimal noise does not effect at all the tessellation, in the sense that all cells remain hexagons. Moreover, even finite-size noise basically does not distort cells in such a way that figures other than hexagons are created. We have not observed non $n = 6$ cells for up to $\alpha \approx 0.12$ in any member of the ensemble. This has been confirmed also considering larger densities (e.g. $\rho_0 = 1000000$). It is more precise, though, to frame the structural stability of the hexagon tessellation in probabilistic terms: the creation of a non-hexagons is very unlikely for the considered range. Since the presence of a Gaussian noise induces for each point x_i a probability distribution in space with—an unrealistic—non-compact support, it is possible to have low-probability outliers that, at local level, can distort heavily the tessellation. Anyway, for all values of α we have that $\langle \mu(n)|_\alpha \rangle = 6$ within few permils, as imposed by the Euler's theorem. For $\alpha > 0.12$, $\langle \sigma(n)|_\alpha \rangle$ is positive and increases monotonically with α; this is accompanied by a monotonic decrease with α of the fraction of hexagons, which are nevertheless dominant for all values of α. For $\alpha > 0.5$ the value of $\langle \sigma(n)|_\alpha \rangle$ is not distinguishable from what obtained for perturbed square and triangular tessellations, This implies that from a statistical point of view, the variable n loses memory of its unperturbed state already for a rather low amount of Gaussian noise, well before becoming indistinguishable from the fully random Poisson case.

3.2 Area and Perimeter of the Cells

For all of the perturbed regular tessellation considered in this study, the parametric dependence on α of the statistical properties of the area of the Voronoi cells is more regular than for the case of the number of sides. Results are shown in Figs. 2a–2b.

In general, the ensemble mean value $\langle \mu(A)|_\alpha \rangle$ of the area of the Voronoi cells is, basically by definition, constrained to be $\rho_0 \langle \mu(A)|_\alpha \rangle = 1$ for all values of α, whereas for all perturbed tessellation the fluctuations $\delta[\mu(A)|_\alpha]$ increase with α and reach for $\alpha > 3$ an asymptotic value, coinciding with that observed in the Poisson-Voronoi case. The α-dependence of $\langle \sigma(A)|_\alpha \rangle$ is more interesting. We first note that the functions $\langle \sigma(A)|_\alpha \rangle$ computed from the three perturbed tessellation are very similar, and the same occurs for $\delta[\sigma(A)|_\alpha]$. This implies that the impact of adding noise in the system in the variability of the area of the cells is

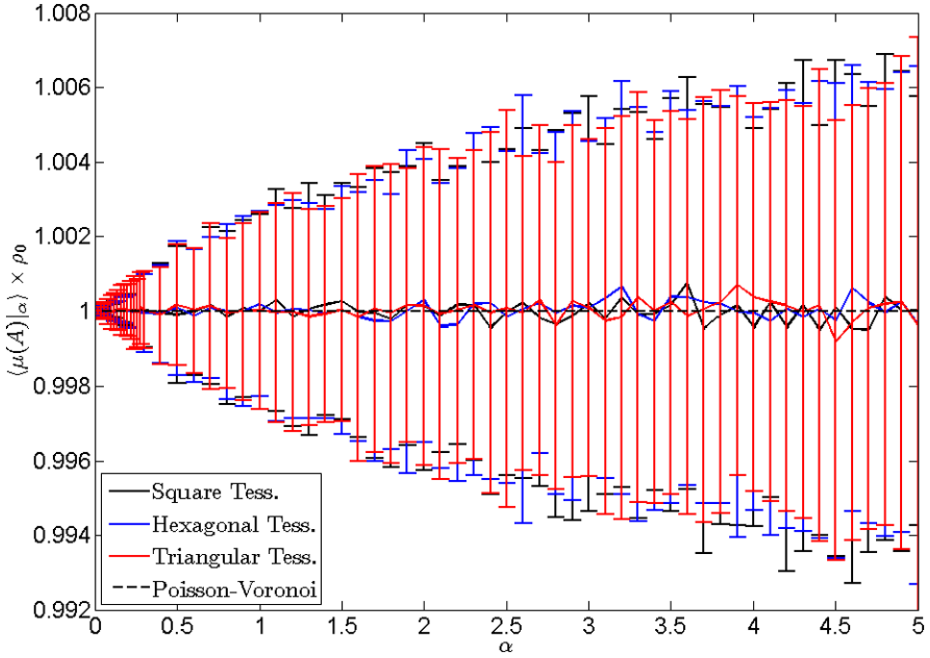

(a)

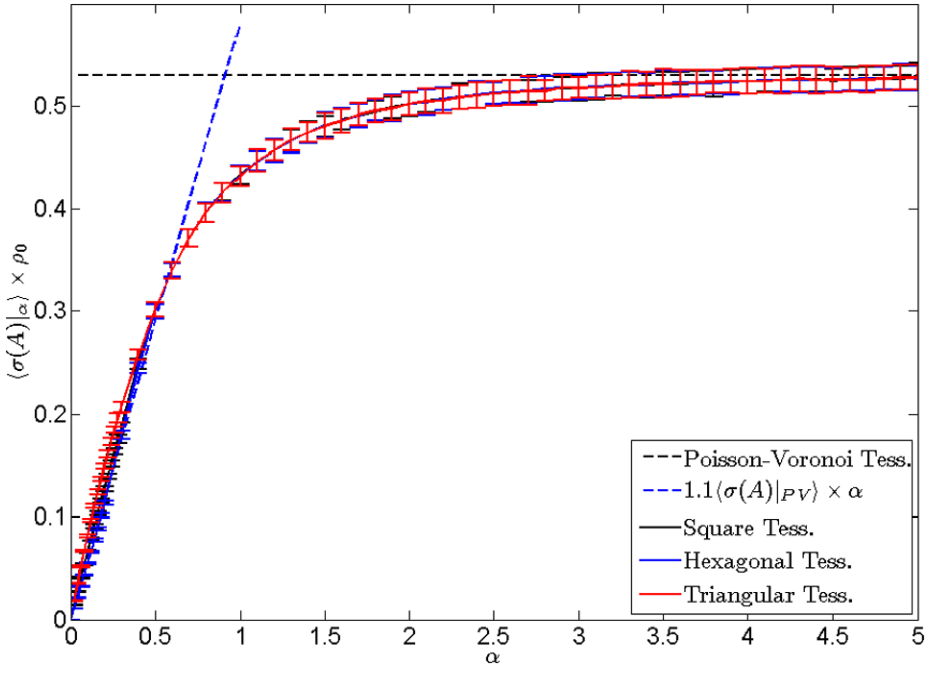

(b)

Fig. 2 (Color online) Ensemble mean of the mean: (**a**) and of the standard deviation; (**b**) of the area (A) of the Voronoi cells. Half-width of the error bars is twice the standard deviation computer over the ensemble. Poisson-Voronoi limit is indicated. In (**b**), linear approximation for small values of α is also shown. Values are multiplied times ρ_0 in order to give universality to the ensemble mean results

quite general and does not depend on the unperturbed patterns. We can be confident of the generality of this result also because for relatively small values of α (say, $\alpha < 0.5$), $\langle \sigma(A)|_\alpha \rangle$ has a specific functional form reminding of symmetry breaking behavior: in such a range we have that $\langle \sigma(A)|_\alpha \rangle \approx 1.1 \langle \sigma(A)|_{PV} \rangle \times \alpha$. The agreement with a linear approximation is worse for the triangular tessellation case. For $\alpha > 2$, $\langle \sigma(A)|_\alpha \rangle$ is almost indistinguishable from the Poisson-Voronoi value, so that we can estimate an asymptotic value $\rho_0 \langle \sigma(A)|_{PV} \rangle \approx 0.53$.

Results for the statistical estimators of the perimeter of the Voronoi cells are shown in Figs. 3a–3b. When considering the perturbed square tessellation, $\langle \mu(P)|_\alpha \rangle$ basically coincides with that of the Poisson-Voronoi case for $\alpha > 1$. Note that also $\sqrt{\rho_0} \langle \mu(P)|_{\alpha=0} \rangle = 4$, which also agrees with the asymptotic Poisson-Voronoi limit. Anyway $\langle \mu(P)|_\alpha \rangle$ is a function with some interesting structure: for $\alpha = \alpha_m \approx 0.25$, $\langle \mu(P)|_\alpha \rangle$ features a distinct minimum $\langle \mu(P)|_{\alpha=\alpha_m} \rangle \approx 0.975 \langle \mu(P)|_V \rangle$, whereas for $\alpha = \alpha_M \approx 0.75$ a maximum for $\langle \mu(P)|_\alpha \rangle$ is realized, with $\langle \mu(P)|_{\alpha=\alpha_M} \rangle \approx 1.01 \langle \mu(P)|_V \rangle$. The unperturbed honeycomb hexagonal tessellation is optimal in the sense of perimeter-to-area ratio, and, when noise is added, the corresponding function $\langle \mu(P)|_\alpha \rangle$ increases quadratically (not shown) with α for $\alpha < 0.3$, whereas for $\alpha > 0.5$ its value coincides with what obtained starting from the regular square tessellation. Finally, in the case of triangular tessellation, the unperturbed case features the largest perimeter-to-area ratio, which is strongly reduced as soon as the noise is switched on, so that a relative minimum is then obtained again for $\alpha = \alpha_{\bar{m}} \approx 0.5$, with $\langle \mu(P)|_{\alpha=\alpha_{\bar{m}}} \rangle \approx 1.05 \langle \mu(P)|_{PV} \rangle$. For $\alpha > 0.6$ the value of the function $\langle \mu(P)|_\alpha \rangle$ basically coincides with those resulting from the two other tessellations.

We deduce that there is, counter-intuitively, a specific amount of noise which optimizes the mean perimeter-to-area ratio for the two unstable regular tessellation—corresponding to $\alpha = \alpha_m$ for the square one and to $\alpha = \alpha_{\bar{m}}$ for the triangular one—whereas, for $\alpha = \alpha_M$ the opposite is realized for all tessellations. When considering the functions $\langle \sigma(P)|_\alpha \rangle$, we are in a similar situation as for the statistics of mean cells area: the result of the impact of noise is the same for all tessellations. For $\alpha < 0.5$, $\langle \sigma(P)|_\alpha \rangle$ is proportional to α, with $\langle \sigma(P)|_\alpha \rangle \approx 1.05 \langle \sigma(P)|_{PV} \rangle \times \alpha$; also in this case the triangular tessellation has a worse agreement with this low-noise approximation. Moreover, for $\alpha > 2$, $\langle \sigma(P)|_\alpha \rangle$ becomes indistinguishable from the asymptotic value realized for Poisson-Voronoi process, given by $\sqrt{\rho_0} \langle \sigma(P)|_{PV} \rangle \approx 0.98$.

3.2.1 Area and Perimeter of n-Sided Cells

A subject of intense investigation has been the characterization of the geometrical properties of n-sided cells; see [20] and references therein for a detailed discussion. We have then computed the for the considered range of α the quantities $\langle \mu(A)|_\alpha \rangle_n$, $\delta[\mu(A)|_\alpha]_n$, $\langle \mu(P)|_\alpha \rangle_n$, and $\delta[\mu(P)|_\alpha]_n$, obtained by stratifying the outputs of the ensemble of simulations with respect to the number of sides n of the resulting cells. The 2-standard deviation confidence interval centered around the ensemble mean is shown as a function of n in Figs. 4a–4b for the area and the perimeter of the cells, respectively, for selected values of α. Note that for larger values of n the error bar is larger because the number of occurrences of n-sided cells is small.

The results of the three perturbed regular tessellations basically agree for $\alpha > 0.5$, thus confirming what shown previously. In particular, for $\alpha > 2$, the results coincide with what resulting from the Poisson-Voronoi case. In this regime, we verify the Lewis law [24], *i.e.* $\langle \mu(A)|_\alpha \rangle_n \approx a_1/\rho_0(n + a_2)$. Our data give $a_1 \approx 0.23$, which is slightly less than what resulting from the asymptotic computation by Hilhorst [19], who obtained a linear coefficient of 0.25. Secondly, and, more interestingly, we confirm that Desch's law [11] is

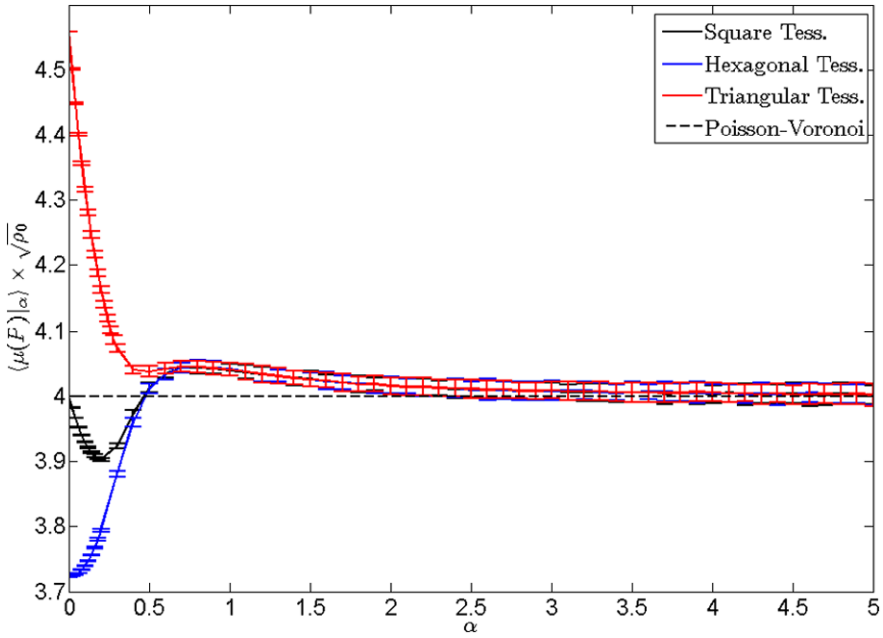

(a)

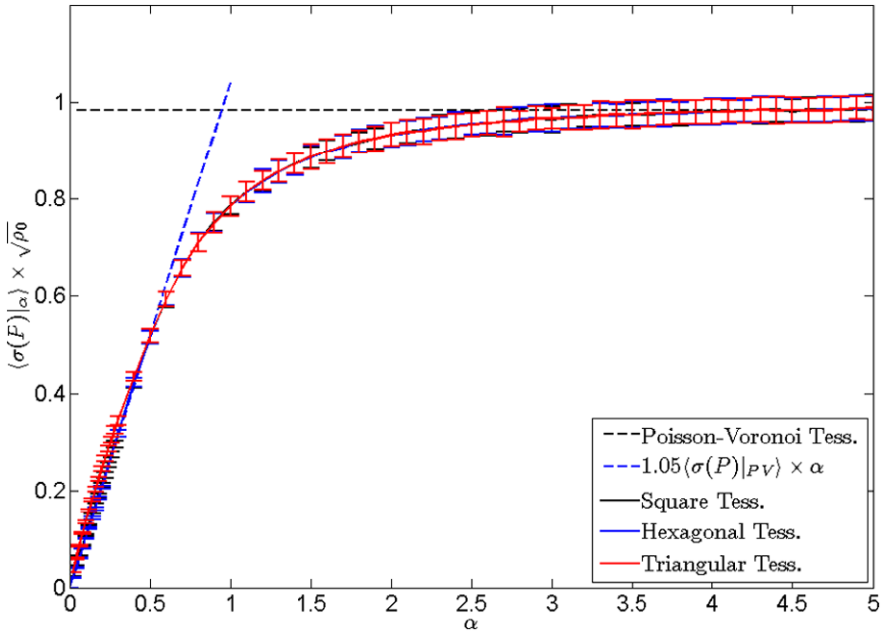

(b)

Fig. 3 (Color online) Ensemble mean of the mean: (**a**) and of the standard deviation; (**b**) of the perimeter (P) of the Voronoi cells. Half-width of the error bars is twice the standard deviation computer over the ensemble. Poisson-Voronoi limit is indicated. In (**b**), linear approximation for small values of α is also shown. Values are multiplied times $\rho_0^{1/2}$ in order to give universality to the ensemble mean results

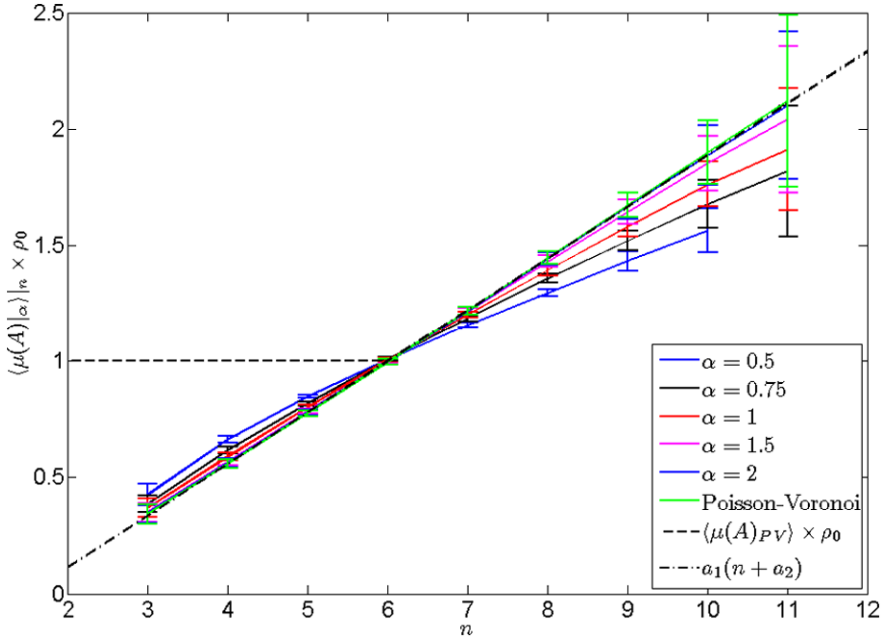

(a)

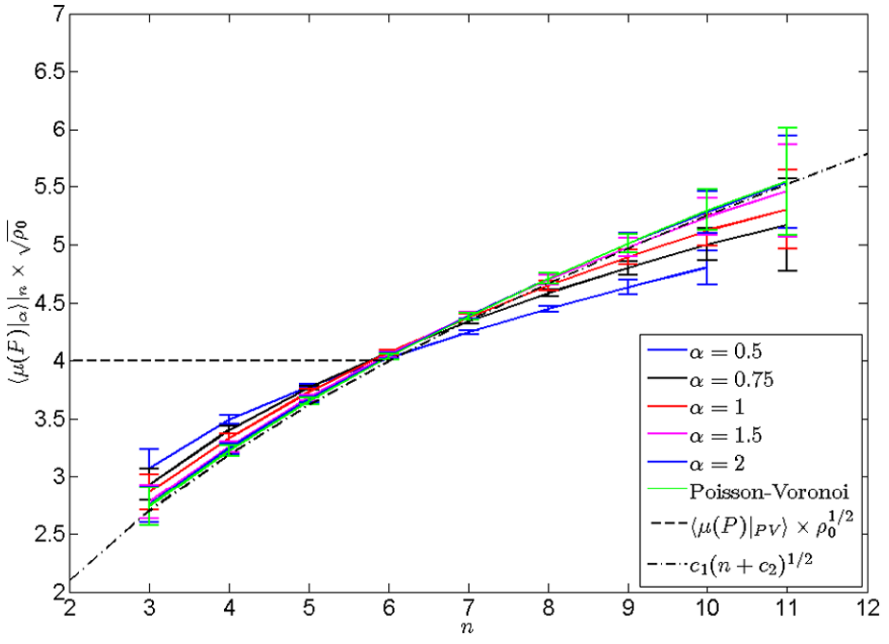

(b)

Fig. 4 (Color online) Ensemble mean of the area A: (**a**) and of the perimeter P; (**b**) of n-sided Voronoi cells. Half-width of the error bars is twice the standard deviation computer over the ensemble. Full ensemble mean is indicated. Linear (**a**) and square root (**b**) fits of the Poisson-Voronoi limit results as a function of n is shown. Values are multiplied times ρ_0 (**a**) and $\rho_0^{1/2}$ (**b**) in order to give universality to the ensemble mean results. See also Fig. 5

violated, *i.e.* $\langle \mu(P)|_\alpha \rangle_n \neq b_1(n+b_2)$, as shown, e.g. by Zhu [39]. Nevertheless, instead of a polynomial dependence on n, we find that a square root law can be established, i.e. $\langle \mu(P)|_\alpha \rangle_n \approx c_1/\sqrt{\rho_0}(\sqrt{n+c_2})$. Our data give $c_1 \approx 1.71$, again slightly less than the asymptotic computation by Hilhorst [19], who obtained $c_1 = \sqrt{\pi} \approx 1.77$. We note that the Lewis law and such law allow the establishment of a weakly n-dependent relationship such as $\langle \mu(A)|_\alpha \rangle_n \propto [\langle \mu(P)|_\alpha \rangle_n]^2$, which is re-ensuring and self-consistent at least in terms of dimensional analysis. Moreover, this agrees with the asymptotic result for large n, $\langle \mu(A)|_\alpha \rangle_n = \frac{1}{4\pi}[\langle \mu(P)|_\alpha \rangle_n]^2$, which derives from the fact that, as shown in [19], cells with many sides tend to have a circular shape.

In the intermediate range ($0.5 < \alpha < 2$), we have that the Lewis law and the square root law are not verified, and, quite naturally, the functions $\langle \mu(A)|_\alpha \rangle_n$ and $\langle \mu(P)|_\alpha \rangle_n$ get more and more similar to their Poisson-Voronoi counterparts as α increases.

An interesting result is that, for $\alpha > 1$, $\rho_0 \langle \mu(A)|_\alpha \rangle_{n=6}$ agrees within statistical uncertainty of few permils with $\rho_0 \langle \mu(A)|_\alpha \rangle = 1$. This implies that $a_1(6+a_2) \approx 1 \Rightarrow a_2 \approx \frac{1}{a_1} - 6 \approx -1.65$. Similarly, for $\alpha > 1$, $\sqrt{\rho_0}\langle \mu(P)|_\alpha \rangle_{n=6}$ constitutes an excellent approximation within 1% to $\sqrt{\rho_0}\langle \mu(P)|_\alpha \rangle$, whose value, as shown in Fig. 3a, is rather close to 4 for $\alpha > 1$, but agreement within statistical uncertainty is basically not found, except, marginally, for very large values of α. This implies that $c_1\sqrt{6+c_2} \approx 4 \Rightarrow c_2 \approx (\frac{4}{c_1})^2 - 6 \approx -0.49$. The validity of these approximate equalities is highlighted in Fig. 5. The ensemble mean estimators restricted to the non-hexagonal polygons are instead heavily biased (positive bias for $n > 6$ and negative bias for $n < 6$). The fact that the ensemble mean of the area and perimeter of the Voronoi cells is so accurately approximated when selecting only the most probable state from a topological point of view—hexagons—is surely striking, also because in the considered range hexagons are dominant but other polygons are also well-represented. In fact, for, *e.g.* $\alpha > 1$, the density of hexagons is smaller than the sum of the densities of pentagons and heptagons.

3.3 Fitting the Probability Density Functions

In agreement with the findings by Zhu et al. [39] for a different parametric investigation of 2D Voronoi cells, we have that for $\alpha > 0$, the empirical pdfs of cells area and perimeter can be fitted with great precision using 2-parameter gamma distributions normalized to 1:

$$f(Y;k,\theta) = Y^{k-1}\frac{\exp[-Y/\theta]}{\theta^k \Gamma(k)} \tag{1}$$

where $Y = P$, A is a continuous variable, k and $\Gamma(k)$ are positive parameters, and $\Gamma(k)$ is the usual gamma function evaluated at k. We consider $\langle k(Y)|_\alpha \rangle$ and $\langle \theta(Y)|_\alpha \rangle$, which are the ensemble means of the best fits of the gamma distribution parameters k and θ for the variable Y. Since in the three cases considered of perturbed tessellations at leading order we have that $\langle \mu(Y)|_\alpha \rangle = \langle k(Y)|_\alpha \theta(Y)|_\alpha \rangle \approx \langle k(Y)|_\alpha \rangle \langle \theta(Y)|_\alpha \rangle$ is constant and $\langle \sigma^2(Y)|_\alpha \rangle = \langle k(Y)|_\alpha \theta^2(Y)|_\alpha \rangle \approx \langle k(Y)|_\alpha \rangle \langle \theta^2(Y)|_\alpha \rangle \propto \alpha^2$ for small values of α, we derive that $\langle k(Y)|_\alpha \rangle \propto \alpha^{-2}$ and $\langle \theta(Y)|_\alpha \rangle \propto \alpha^2$, so that their values change by orders of magnitude as noise is switched on.

Hilhorst [19] has proved in the case of Poisson-Voronoi processes that the asymptotic behavior the pdf of the number of sides n of Voronoi cells is not compatible with any discrete (basically such that Y in (1) takes integer values) gamma distribution model. Nevertheless, in agreement with the findings of Tanemura [32], we find that for Poisson-Voronoi processes discrete gamma models provide excellent fits of the empirical pdfs. It may be argued that

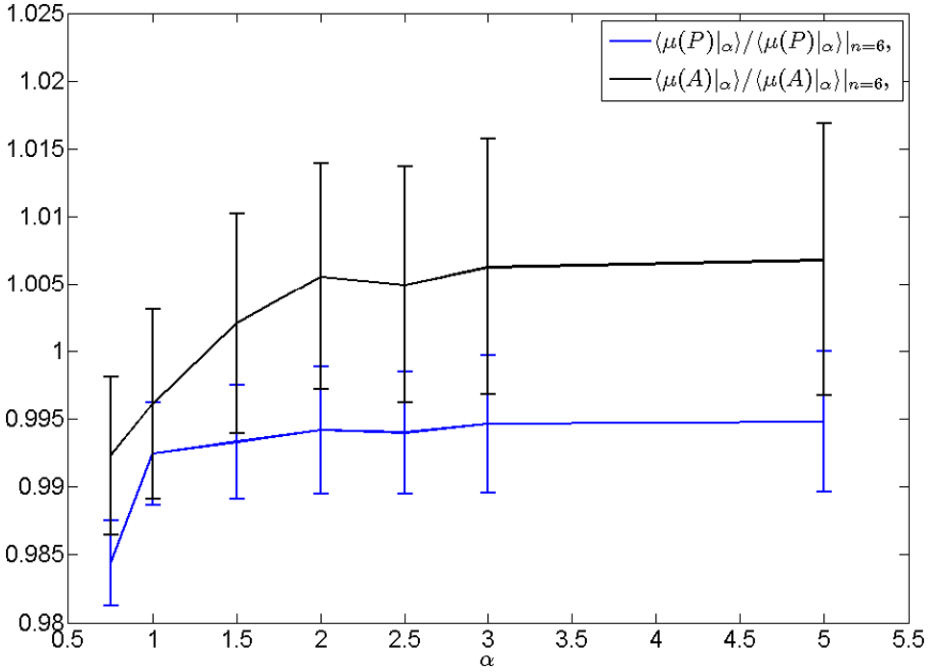

Fig. 5 (Color online) Agreement between the ensemble mean of the area A of the perimeter P of hexagonal Voronoi cells and the full ensemble mean. Half-width of the error bars is twice the standard deviation computer over the ensemble

the asymptotic behavior becomes relevant only for very high values of n, which are seldom obtained with actual simulations. Moreover, discrete gamma distribution models work very well for all the considered non-singular cases—$\alpha > 0$, for perturbed triangular and rectangular tessellations and, within the numerical precision reached in this experiments, for $\alpha > 0.12$ when considering perturbed hexagonal tessellation.

4 Summary and Conclusions

This numerical study wishes to bridge the properties of the regular square, hexagonal, and triangular Voronoi tessellations of the plane to those generating from Poisson point processes, thus analyzing in a common framework symmetry breaking processes and the approach to uniformly random distributions. This is achieved by resorting to a simple parametric form of random perturbations driven by a Gaussian noise to the positions of the points around which the Voronoi tessellation is created. The standard deviation of the position of the points induced by the Gaussian noise is expressed as $|\varepsilon| = \alpha/\sqrt{\rho_0}$, where α is the control parameter, ρ_0 is the coarse-grained density of tessellation generating points, and $1/\sqrt{\rho_0}$ is the natural length scale. We consider as starting points the regular square, honeycomb hexagonal, and triangular tessellations, and change the value of α from 0, where noise is absent, up to 5. In this way, the probability distribution of points is in all cases periodic. For each value of α, we perform a set of simulations, in order to create an ensemble of points

and of corresponding Voronoi tessellation in the unit square, and compute the statistical properties of n, A, and P, the number of sides, the area and the perimeter of the resulting cell, respectively. The main results we obtain can be listed as follows:

- The symmetry breaking induced by the introduction of noise destroys the square and triangular tessellations, which are structurally unstable: already for an infinitesimal amount of noise a sharp transition occur, so that the ensemble mean of the mean and of the standard deviation of the number of sides have a discontinuity, finite ensemble fluctuations appear, and the most common polygons turn out to be hexagons.
- Instead, the honeycomb hexagonal tessellation is very stable and all Voronoi cells are found to be hexagon for finite noise up within a certain range of $\alpha (\alpha < 0.12)$.
- The statistical properties of the number of sides of the Voronoi cells resulting from perturbed square and triangular tessellations are approximately constant for a finite range of α ($0 < \alpha < 0.35$ for the square and $0 < \alpha < 0.45$ for the triangular case, respectively), This property seems to define robustly a topologically quasi-stable weakly perturbed state.
- Interesting signatures of symmetry breaking emerge from a linear relationship between the standard deviation of the perimeter and the area of the Voronoi cells and the parameter α for small values of α for all sorts of tessellations analyzed; in general, the ensemble mean of the standard deviations of these quantities monotonically increase with α, in agreement with the changeover towards a more extreme random nature of the tessellation.
- Already for a moderate amount of Gaussian noise (say $\alpha > 0.5$), memory of the specific initial unperturbed state is lost, because the statistical properties of the three perturbed regular tessellations are indistinguishable.
- In the case of perturbed square (triangular) tessellation, for a specific intensity of the noise determined by $\alpha = \alpha_m \approx 0.25$ ($\alpha = \alpha_m \approx 0.5$), it is possible to minimize the mean perimeter-to-area ratio of the Voronoi cells, whereas by choosing $\alpha = \alpha_M \approx 0.75$ we obtain a relative maximum for perimeter-to-area ratio for all perturbed tessellations.
- For large values of α (*e.g.* $\alpha > 2$), quite expectedly, the statistical properties of the perturbed regular tessellations converge, both in terms of ensemble mean and fluctuations, to those of the Poisson Voronoi process with the same intensity, since the points generating the tessellations are from a practical point of view randomly and uniformly distributed in the plane.
- For all values of $\alpha > 0$, the 2-parameter gamma distribution family does a great job in providing excellent models for fitting the distribution of sides, area, perimeters of the Voronoi cells, the only exceptions being the singular distributions obtained for n in the case of perturbed honeycomb tessellation for $\alpha < 0.12$. This is especially surprising as in the case of Poisson-Voronoi processes we have theoretical evidence showing that 2-parameter discrete gamma models are not compatible with the asymptotic behavior of the pdf of the number of sides of the Voronoi cells [19]. The reason why, practically speaking, the 2-parameter gamma distribution functions constitute such efficient fitting models for both the continuous and discrete variables considered here is still unclear.
- The geometrical properties of n-sided cells change with α until the Poisson-Voronoi limit is reached for $\alpha > 2$; in this limit the Desch law for perimeters is confirmed to be not valid and a square root dependence on n, which allows an easy link to the Lewis law for areas, is established.
- The ensemble mean of the cells area and perimeter restricted to the hexagonal cells provides a striking approximation to the full ensemble mean for $\alpha > 1$; this reinforces the idea that hexagons, apart from their bare numerical prominence, can be taken as *typical* polygons in 2D Voronoi tessellations.

In previous works much larger densities of points have been considered—up to several million [32]. In this work, those numbers would be rather inconvenient because we perform a parametric study of ensemble runs. Nevertheless, we wish to emphasize that whereas, as discussed in the text, the choice of ρ_0 does not alter any of the result on the ensemble mean of statistical properties of the intensive quantities n, A, and P, larger values of ρ_0 would allow for smaller ensemble fluctuations. A related benefit of using larger values of ρ_0 is the possibility of computing the statistics on n-sided cells on a larger number of classes of polygons, since the probability of detecting a n-sided polygons decreases very quickly with n.

A topic that has been left aside in the present work is the study of the joint statistical properties of the number of sides of neighboring cells. This matter is especially worth exploring given the recent explanation of the violation of the Aboav's law for Poisson-Voronoi tessellations [20].

The results here described may be useful in understanding the mechanical (and maybe electronic) properties of graphene, which has recently received a great deal of attention as first example of truly atomic 2D crystalline matter [16]. In fact, in graphene atoms are positioned in a regular hexagonal honeycomb structure and therefore the Voronoi tessellation is given, as explained in Sect. 2, by regular triangles. We have shown in this work that such tessellation is rather peculiar as it maximizes the perimeter-to-area ratio of the Voronoi cells and its topology is unstable with respect to infinitesimal dislocations of the initial points, thus being affected by vibrational motions and defects.

Finally, we believe that it is definitely worthy to extend this study to the 3D case, which might be especially significant for solid-state physics applications, with particular regard to crystals' defects and electronic impacts of vibrational motion in various discrete rotational symmetry classes [5]. The analysis of the properties of the various cubic crystalline structure is especially promising. Nevertheless, a much larger computational cost has to be expected, since a larger number of points and a larger computing time per point are required for sticking to the same precision in the evaluation of the statistical properties.

Acknowledgements The author wishes to thank F. Bassani, R. Benzi, A. Speranza for stimulating conversations and one anonymous reviewer for providing useful insights for increasing the quality of the paper.

References

1. Ashcroft, N.W., Mermin, N.D.: Solid State Physics. Saunders, Philadelphia (1976)
2. Aurenhammer, F.: Voronoi diagrams—a survey of a fundamental geometric data structure. ACM Comput. Surv. **23**, 345–405 (1991)
3. Barber, C.B., Dobkin, D.P., Huhdanpaa, H.T.: The quickhull algorithm for convex hulls. ACM Trans. Math. Softw. **22**, 469–483 (1996)
4. Barrett, T.M.: Voronoi tessellation methods to delineate harvest units for spatial forest planning. Can. J. For. Res. **27**(6), 903–910 (1997)
5. Bassani, F., Pastori-Parravicini, G.: Electronic States and Optical Transitions in Solids. Pergamon, Oxford (1975)
6. Bennett, L.H., Kuriyama, M., Long, G.G., Melamud, M., Watson, R.E., Weinert, M.: Local atomic environments in periodic and aperiodic Al–Mn alloys. Phys. Rev. B **34**, 8270–8272 (1986)
7. Bowyer, A.: Computing Dirichlet tessellations. Comput. J. **24**, 162–166 (1981)
8. Calka, P.: Precise formulae for the distributions of the principal geometric characteristics of the typical cells of a two-dimensional Poisson Voronoi tessellation and a Poisson line process. Adv. Appl. Probab. **35**, 551–562 (2003)
9. Christ, N.H., Friedberg, R., Lee, T.D.: Random lattice field theory: general formulation. Nucl. Phys. B **202**, 89–125 (1982)
10. Delaunay, B.: Sur la sphère vide. Otd. Mat. Estestv. Nauk **7**, 793–800 (1934)

11. Desch, C.H.: The solidification of metals from the liquid state. J. Inst. Metals **22**, 241 (1919)
12. Dotera, T.: Cell crystals: Kelvin's polyhedra in block copolymer melts. Phys. Rev. Lett. **82**, 105–108 (1999)
13. Drouffe, J.M., Itzykson, C.: Random geometry and the statistics of two-dimensional cells. Nucl. Phys. B **235**, 45–53 (1984)
14. Finch, S.R.: Mathematical Constants. Cambridge University Press, Cambridge (2003)
15. Finney, J.L.: Volume occupation, environment and accessibility in proteins. The problem of the protein surface. J. Mol. Biol. **96**, 721–732 (1975)
16. Geim, A.K., Novoselov, K.S.: The rise of graphene. Nat. Mater. **6**, 183–191 (2007). doi:10.1038/nmat1849
17. Goede, A., Preissner, R., Frömmel, C.: Voronoi cell: new method for allocation of space among atoms: elimination of avoidable errors in calculation of atomic volume and density. J. Comput. Chem. **18**, 1113–1118 (1997)
18. Han, D., Bray, M.: Automated Thiessen polygon generation. Water Resour. Res. **42**, W11502 (2006). doi:10.1029/2005WR004365
19. Hilhorst, H.J.: Asymptotic statistics of the n-sided planar Poisson–Voronoi cell, I: exact results. J. Stat. Mech. P09005 (2005). doi:10.1088/1742-5468/2005/09/P09005
20. Hilhorst, H.J.: Planar Voronoi cells: the violation of Aboav's law explained. J. Phys. A: Math. Gen. **39**, 7227–7243 (2006). doi:10.1088/0305-4470/39/23/004
21. Hinde, A.L., Miles, R.E.: Monte Carlo estimates of the distributions of the random polygons of the Voronoi tessellation with respect to a Poisson process. J. Stat. Comput. Simul. **10**, 205–223 (1980)
22. Icke, V.: Particles, space and time. Astrophys. Space Sci. **244**, 293–312 (1996)
23. Kumar, S., Kurtz, S.K., Banavar, J.R., Sharma, M.G.: Properties of a three-dimensional Poisson–Voronoi tessellation: a Monte Carlo study. J. Stat. Phys. **67**, 523–551 (1992)
24. Lewis, F.T.: The correlation between cell division and the shapes and sizes of prismatic cells in the epidermis of Cucumis. Anat. Rec. **38**, 341–376 (1928)
25. Lucarini, V., Danihlik, E., Kriegerova, I., Speranza, A.: Does the Danube exist? Versions of reality given by various regional climate models and climatological data sets. J. Geophys. Res. **112**, D13103 (2007). doi:10.1029/2006JD008360
26. Meijering, J.L.: Interface area, edge length, and number of vertices in crystal aggregates with random nucleation: Phillips research reports. Philips Res. Rep. **8**, 270–290 (1953)
27. Okabe, A., Boots, B., Sugihara, K., Chiu, S.N.: Spatial Tessellations—Concepts and Applications of Voronoi Diagrams, 2nd edn. Wiley, New York (2000)
28. Rapaport, D.C.: Hexagonal convection patterns in atomistically simulated fluids. Phys. Rev. E **73**, 025301 (2006)
29. Senthil Kumar, V., Kumaran, V.: Voronoi neighbor statistics of hard-disks and hard-spheres. J. Chem. Phys. **123**, 074502 (2005)
30. Sortais, M., Hermann, S., Wolisz, A.: Analytical investigation of intersection-based range-free localization information gain. In: Proc. of European Wireless (2007)
31. Tanemura, M., Ogawa, T., Ogita, N.: A new algorithm for three-dimensional Voronoi tessellation. J. Comput. Phys. **51**, 191–207 (1983)
32. Tanemura, M.: Statistical distributions of Poisson-Voronoi cells in two and three dimensions. Forma **18**, 221–247 (2003)
33. Thiessen, A.H., Alter, J.C.: Climatological data for July, 1911: district No. 10, Great Basin. Monthly Weather Review, July, 1082–1089 (1911)
34. Tsai, F.T.-C., Sun, N.-Z., Yeh, W.W.-G.: Geophysical parameterization and parameter structure identification using natural neighbors in groundwater inverse problems. J. Hydrol. **308**, 269–283 (2004)
35. Voronoi, G.: Nouvelles applications des paramètres continus à la théorie des formes quadratiques. Premier mémoire: sur quelques propriétées des formes quadritiques positives parfaites. J. Reine Angew. Math. **133**, 97–178 (1907)
36. Voronoi, G.: Nouvelles applications des parametres continus a la theorie des formse quadratiques. Duesieme memoire: recherches sur les parallelodres primitifs. J. Reine Angew. Math. **134**, 198–287 (1908)
37. Watson, D.F.: Computing the n-dimensional tessellation with application to Voronoi polytopes. Comput. J. **24**, 167–172 (1981)
38. Weaire, D., Kermode, J.P., Wejchert, J.: On the distribution of cell areas in a Voronoi network. Philos. Mag. B **53**, L101–L105 (1986)
39. Zhu, H.X., Thorpe, S.M., Windle, A.H.: The geometrical properties of irregular two-dimensional Voronoi tessellations. Philos. Mag. A **81**, 2765–2783 (2001)